# Photochemical Activation of C–H Bonds on a Rhodium Catalyst. Observation of a Competitive Effect on the Surface

**Jason C. S. Wong and John T. Yates, Jr.***

*Contribution from the University of Pittsburgh, Department of Chemistry, Surface Science Center, Pittsburgh, Pennsylvania 15260*

*Received May 21, 1993. Revised Manuscript Received August 6, 1993®*

**Abstract:** The UV (325 nm) photolysis of the $Rh^1(CO)_2$ species on an $Al_2O_3$ support produces an active surface intermediate, $Rh^1(CO)$, which reacts with the C–H bond of cyclohexane by oxidative addition to form a postulated surface species, $Rh(CO)(H)(C_6H_{11})$. This species degrades to form a stable $C_6H_{11}$ species on the surface. Unexpectedly, the normalized yield of surface $C_6H_{11}$ species was found to be higher for lower Rh loadings using the same number of UV photons per unit area. This could be qualitatively explained by the fact that the formation of a dimer surface species, $Rh_2(CO)_3$ (a competitive reaction for the intermediate, $Rh^1(CO)$, responsible for C–H bond activation), is favored for high surface concentrations of $Rh^1(CO)_2$. It is shown that the dimer formation competes with the desired C–H bond activation process.

## I. Introduction

Because of the chemical inertness of alkanes and the possibility of using methane in natural gas as a carbon source for petrochemicals, the activation of C–H bonds in alkanes is of current interest.

Recently, we reported[1,2] that the C–H bonds in cyclohexane can be activated by a postulated 16-electron unstable surface intermediate, $Rh^1(CO)$ (II), which is formed during the ultraviolet (UV) photodecomposition of $Rh^1(CO)_2$ (I) supported on an alumina ($Al_2O_3$) surface. The product is a presumed unstable surface species, $Rh(H)(CO)(C_6H_{11})$ (III), which yields a stable cyclohexyl surface species, $C_6H_{11}(a)$ (IV), probably adsorbed on the $Al_2O_3$ support.

$$\underset{\mathbf{I}}{Rh^1(CO)_2} \xrightarrow{h\nu,\,-CO} \underset{\mathbf{II}}{Rh^1(CO)} \xrightarrow{C_6H_{12}} \underset{\mathbf{III}}{Rh(H)(CO)(C_6H_{11})} \rightarrow \underset{\mathbf{IV}}{C_6H_{11}(a)} \quad (1)$$

In this report, using high sensitivity transmission infrared spectroscopy, the formation and UV photodecomposition of $Rh^1(CO)_2$ and the production of surface cyclohexyl species has been monitored quantitatively as a function of UV exposure and as a function of the magnitude of the rhodium concentration on the alumina support surface.

The chemistry of $Rh^1(CO)_2$, the rhodium *gem*-dicarbonyl species, has been well-studied in the past[3-28] using infrared spectroscopy (IR), X-ray photoelectron spectroscopy (XPS), extended X-ray absorption fine structure (EXAFS), and mass spectroscopy-temperature programmed reaction (MS-TPR). It is now generally accepted that when CO chemisorbs on Rh metal supported on oxide surfaces, CO causes the partial disintegration of Rh crystallites into isolated single Rh atoms which eventually form the *gem*-dicarbonyl species, $Rh^1(CO)_2$.[3,6] In addition to the "isolated" $Rh^1(CO)_2$, two other adsorbed CO species, terminal and bridging CO, are also formed on the surface of non-disrupted Rh crystallites. The $Rh^1(CO)_2$ species exhibits a characteristic sharp IR doublet at 2103 and 2034 $cm^{-1}$, assigned respectively to the coupled symmetric and antisymmetric C–O stretching modes. A distinctive feature of this doublet is that the IR frequencies are independent of CO coverage,[6] supporting the idea that $Rh^1(CO)_2$ is atomically dispersed on the alumina surface preventing vibrational interaction between neighboring $Rh^1(CO)_2$ species. On the other hand, the IR frequencies of terminal and bridging CO on Rh crystallites shift upward with increasing coverage of CO.

The adsorbate-induced structural change in this system was further confirmed by EXAFS results which showed that the Rh–Rh coordination number decreases after the CO chemisorption.[18,19] The oxidation of $Rh^0$ to $Rh^{1+}$ during the *gem*-dicarbonyl formation was proven by XPS studies which showed a shift of binding energy of the Rh(3d) electrons to a higher energy when CO chemisorbs on oxide-supported Rh.[18-20] It was postulated that the isolated hydroxyl group (Al–OH) on oxide surfaces is the oxidizing agent responsible for the oxidation of $Rh^0$ to $Rh^{1+}$.[21-28] This was supported by the following facts: (i) a proportional consumption of isolated Al–OH groups accompanies

• Abstract published in *Advance ACS Abstracts*, January 15, 1994.

(1) Ballinger, T. H.; Yates, J. T., Jr. *J. Phys. Chem.* **1992**, *96*, 9979.
(2) Ballinger, T. H.; Yates, J. T., Jr. *J. Am. Chem. Soc.* **1992**, *114*, 10074.
(3) Yang, A. C.; Garland, C. W. *J. Phys. Chem.* **1957**, *61*, 1504.
(4) Primet, M. *J. Chem. Soc., Faraday Trans. 1* **1978**, *74*, 2570.
(5) Yao, H. C.; Rothschild, W. G. *J. Chem. Phys.* **1978**, *68*, 4774.
(6) Yates, J. T., Jr.; Duncan, T. M.; Worley, S. D.; Vaughan, R. W. *J. Chem. Phys.* **1979**, *70*, 1219.
(7) Yates, J. T., Jr.; Duncan, T. M.; Vaughan, R. W. *J. Chem. Phys.* **1979**, *71*, 3908.
(8) Solymosi, F.; Sarkany, J. *J. Appl. Surf. Sci.* **1979**, *3*, 68.
(9) Solymosi, F.; Erdohelyi, A.; Kocsis, M. *J. Catal.* **1980**, *65*, 428.
(10) Antoniewicz, P. R.; Cavanagh, R. R.; Yates, J. T., Jr. *J. Chem. Phys.* **1980**, *73*, 3456.
(11) Cavanagh, R. R.; Yates, J. T., Jr. *J. Chem. Phys.* **1981**, *74*, 4150.
(12) Rice, C. A.; Worley, S. D.; Curtis, C. W.; Guin, J. A.; Tarrer, A. R. *J. Chem. Phys.* **1981**, *74*, 6487.
(13) Yates, J. T., Jr.; Cavanagh, R. R. *J. Catal.* **1982**, *74*, 97.
(14) Yates, J. T., Jr.; Kolasinski, K. *J. Chem. Phys.* **1983**, *79*, 1026.
(15) Robbins, J. L. *J. Phys. Chem.* **1986**, *90*, 3381.
(16) Duncan, T. M.; Root, T. W. *J. Phys. Chem.* **1988**, *92*, 4426.
(17) Thayer, A. M.; Duncan, T. M. *J. Phys. Chem.* **1989**, *93*, 6763.
(18) van't Blik, H. F. J.; van Zon, J. B. A. D.; Huizinga, T.; Vis, J. C.; Koningsberger, D. C.; Prins, R. *J. Phys. Chem.* **1983**, *87*, 2264.
(19) van't Blik, H. F. J.; van Zon, J. B. A. D.; Huizinga, T.; Vis, J. C.; Koningsberger, D. C.; Prins, R. *J. Am. Chem. Soc.* **1985**, *107*, 3139.
(20) Wong, T. T.; Stakheev, A. Y.; Sachtler W. M. H. *J Phys. Chem.* **1992**, *96*, 7733.
(21) Solymosi, F.; Pasztor, M. *J. Phys. Chem.* **1985**, *89*, 4789.
(22) Solymosi, F.; Pasztor, M. *J. Phys. Chem.* **1986**, *90*, 5312.
(23) Ballinger, T. H.; Yates, J. T., Jr. *J. Phys. Chem.* **1991**, *95*, 1694.
(24) Basu, P.; Panayotov, D.; Yates, J. T., Jr. *J.Phys. Chem.* **1987**, *91*, 3133.
(25) Basu, P.; Panayotov, D.; Yates, J. T., Jr. *J. Am. Chem. Soc.* **1988**, *110*, 2074.
(26) Zaki, M. I.; Kunzmann, G.; Gates, B. C.; Knozinger, H. *J. Phys. Chem.* **1987**, *91*, 1486.
(27) Paul, D. K.; Ballinger, T. H.; Yates, J. T., Jr. *J. Phys. Chem.* **1990**, *94*, 4617.
(28) Zaki, M. I.; Ballinger, T. H.; Yates, J. T., Jr. *J. Phys. Chem.* **1991**, *95*, 4028.

0002-7863/94/1516-1610$04.50/0 

the $Rh^1(CO)_2$ formation;[24,25] (ii) the formation of $Rh^1(CO)_2$ can be inhibited by the removal of isolated Al–OH groups chemically[26–28] or thermally;[21–23] (iii) production of $H_2$ gas (due to the reduction of Al–OH) during $Rh^1(CO)_2$ formation was detected by MS-TPR.[20]

In the photooxidation experiments shown in eq 1, $Rh^1(CO)$(a) (II) and $Rh(H)(CO)(C_6H_{11})$(a) (III) are not detected by IR spectroscopy.[1,2] A series of control experiments[1,2] have been conducted to show the following: (i) at 300 K, only UV light can cause a substantial photodesorption of CO from $Rh^1(CO)_2$ as detected by mass spectrometry (thermal desorption is very insignificant compared to photodesorption at 300 K); (ii) cyclohexane can only be activated in the presence of both CO (i.e., Rh metal does not activate cyclohexane even in the presence of UV light) and UV photons (i.e., $Rh^1(CO)_2$ is not able to activate cyclohexane without UV photons). Thus, photolytically-produced $Rh^1(CO)$ is postulated to be the surface species which activates cyclohexane.

The photochemical reaction of $Rh^1(CO)_2$ supported on alumina with cyclohexane is a surface reaction analogous to that of $(C_5H_5)$-$Rh(CO)_2$ in the gas phase with neopentane,[29] as we have previously reported.[1,2] So it is believed that $Rh^1(CO)$ and $Rh(H)(CO)$-$(C_6H_{11})$ exist as short-lifetime surface species during the photochemical reaction. The distinctive feature of this surface reaction is that the decomposition of the surface $Rh(H)(CO)$-$(C_6H_{11})$ species forms a cyclohexyl surface species which is stable up to 600 K,[1,2] probably because of capture on the $Al_2O_3$ support.

In this work, the effect of Rh loading on alumina on the yield of cyclohexyl surface species formed by the photochemical reaction was investigated by IR spectroscopy. Unexpectedly, high Rh loading yielded *less* cyclohexyl on the surface. This effect is explained by the fact that the unphotolyzed $Rh^1(CO)_2$ competes with the gaseous cyclohexane for the active intermediate, $Rh^1$-$(CO)$, to form a dinuclear surface species, $>Rh_2(CO)_3$, which we have observed by IR spectroscopy. Therefore, as the loading of Rh goes up, more $Rh^1(CO)_2$ is present per unit area enhancing the formation of $Rh_2(CO)_3$ and inhibiting alkane activation.

## II. Experimental Section

The construction and use of the IR cell used in this work has been described previously.[30] Basically, it is a bakeable stainless steel ultra-high-vacuum cell containing KBr windows which are sealed by Viton O-rings which are differentially pumped.

The $Rh/Al_2O_3$ samples were supported on a 0.001 in. thick tungsten grid which is held rigidly via a pair of nickel clamps to the copper rods of a power/thermocouple feedthrough. A chromel/alumel thermocouple was spot-welded on the top-central region of the tungsten mesh, so that the sample temperature can be measured. An electronic temperature controller maintains a constant sample temperature within ±1 K.[31] The sample can be controlled at any temperature from 150 to 1400 K by passing electrical current through the high resistance tungsten grid and using liquid nitrogen coolant.

The IR cell is connected to a stainless steel vacuum system which is pumped by a 60 L/s turbomolecular pump (Balzers TPU060) and a 30 L/s ion pump (Varian 911-5032), so it can reach a base pressure $<1 \times 10^{-8}$ Torr. The vacuum system also contains a differentially pumped quadrupole mass spectrometer (Dycor Electronic Inc. M100M, range: 1-100 amu) for leak checking and gas analysis through a Granville-Phillips leak valve. The pressure of gaseous reactants is measured by a MKS Baratron (116A) capacitance manometer (range: $10^{-3}$–$10^3$ Torr).

The starting materials used to make $Rh/Al_2O_3$ were Degussa Aluminum Oxide C (101 $m^2/g$) and Alfa $RhCl_3 \cdot 3H_2O$. Different loadings of $Rh/Al_2O_3$ samples were prepared by first dissolving appropriate amounts of $RhCl_3 \cdot 3H_2O$ in ~10 mL of distilled water. $Al_2O_3$ was added to the aqueous solution of $RhCl_3$, and then the mixture was agitated in an ultrasonic bath for about 45 min in order to make sure the $Al_2O_3$ is well-dispersed in the slurry. Acetone (100 mL, Mallinckrodt, analytical reagent grade) was then added to form the final mixture. The mixture was then uniformly sprayed by a nitrogen gas pressurized atomizer onto the entire area (5.2 $cm^2$) of the tungsten grid which was held at about 50 °C to flash evaporate the acetone and water during spraying.[30] The net weight of samples sprayed on the tungsten grid was 17.8–37.7 mg (3.4–7.3 mg/$cm^2$).

The sprayed sample was then mounted on the feedthrough in the IR cell followed by evacuation in vacuum and by outgassing at 475 K for 12 h before reduction. Reduction was carried out at 475 K with four exposures (15, 30, 45, and 60 min) of 200 Torr of hydrogen gas (Matheson 99.999% pure); the IR cell was evacuated for 15 min after each exposure. Then the sample was allowed to outgas under vacuum at 475 K for another 12 h.

Infrared spectra were obtained with a purged Perkin-Elmer PE580B double beam grating infrared spectrophotometer coupled with a Perkin-Elmer 3600 data station for data storage and manipulation. The spectra shown here were taken by averaging 4–25 times, depending on the relative signal-to-noise ratio, with 5.3-$cm^{-1}$ resolution and 1 data point per $cm^{-1}$. Difference spectra (alumina background subtracted) are shown except where otherwise specified.

A 350-W high-pressure mercury arc lamp (Oriel Corp. 6286) was used as the UV light source. The lamp is mounted inside a lamp housing (Oriel 66011) equipped with a 600-W power supply, a F/1 two element UV fused silica condensing lens (for light focusing), a water filter (for absorbing the IR radiation), an iris diaphragm (for adjustable light attenuation), and a filter holder which holds a 325 ± 50 nm bandpass filter (Oriel 51650). The photon flux of the filtered UV light as measured by a calibrated[32] EG&G (HUV-4000B) photodiode was $1.1 \times 10^{17}$ photons $cm^{-2}$ $s^{-1}$, with an absolute accuracy of ±10%.

A typical experiment was performed as follows. IR spectra were taken before the exposure to UV light. Then the IR cell was moved out of the IR spectrophotometer without breaking the vacuum. This allows a perfect and direct alignment of the UV lamp to the IR cell. The photon flux was periodically measured with the photodiode placed in the optical location normally occupied by the sample. In addition, the photon flux of the UV light could be monitored continuously during the photoreaction by the photodiode, observing ultraviolet light transmission through the sample, so that a correction could be made for the slight change of photon flux between individual experiments.

The CO (Matheson) was obtained in a break-seal glass bulb with 99.9% purity. The cyclohexane (UV grade, Fluka Chemical Corp., 99.5% purity) was transferred into a glass/metal storage bulb under a nitrogen atmosphere and then purified by several freeze–pump–thaw cycles. Impurity analysis of the cyclohexane by gas chromatography showed that less than 10 ppm of cyclohexene and benzene were present.

## III. Results and Discussion

**A. Activation of Cyclohexane by UV Photolysis of $Rh^1(CO)_2$.** The IR spectrum following the chemisorption of CO on 0.75% $Rh/Al_2O_3$ is shown in Figure 1A. It was obtained by introducing 9.2 Torr of CO into the IR cell containing the reduced $Rh/Al_2O_3$ sample at 300 K for 20 min, followed by evacuation to $<1 \times 10^{-6}$ Torr for 15 min. The spectrum shows that the dominant spectroscopic features on alumina were from $Rh^1(CO)_2$, which is identified by two sharp bands at 2103 and 2034 $cm^{-1}$. These two bands were assigned respectively to the symmetric and the antisymmetric C–O stretching mode of the *gem*-dicarbonyl species.[3] As previously mentioned, the atomically dispersed $Rh^1$-$(CO)_2$ is formed by the disruption of metallic Rh crystallites, $Rh^0_x$, during the chemisorption of CO.[6] A shoulder at 2063 $cm^{-1}$ and a broad band at 1820 $cm^{-1}$ were found in the IR spectrum and were assigned respectively to the terminal and bridging CO chemisorbed on non-disrupted metallic Rh crystallites.[6] Higher loading of Rh enhances these bands due to chemisorption of CO on metallic Rh sites.[11,25]

After the $Rh^1(CO)_2$ was formed on the surface, 2.13 Torr of cyclohexane was introduced into the IR cell. The UV ($\lambda$ = 325 nm, photon flux = $1.1 \times 10^{17}$ photons $cm^{-2}$ $s^{-1}$) photolysis of $Rh^1(CO)_2$ in the presence of cyclohexane was carried out for 5

(29) Wasserman, E. P.; Moore, C. B.; Bergman, R. G. *Science* **1992**, *225*, 315.
(30) Basu, P.; Ballinger, T. H.; Yates, J. T., Jr. *Rev. Sci. Instrum.* **1988**, *59*, 1321.
(31) Muha, R. J.; Gates, S. M.; Yates, J. T., Jr.; Basu, P. *Rev. Sci. Instrum.* **1985**, *56*, 613.
(32) Hanley, L.; Guo, X.; Yates, J. T., Jr. *J. Chem. Phys.* **1989**, *91*, 7220.

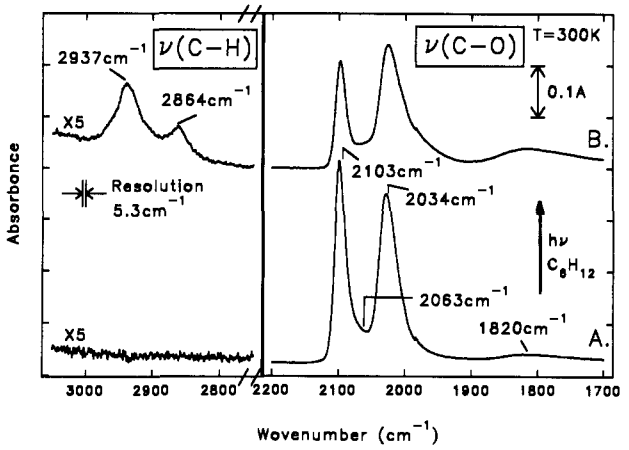


**Figure 1.** Infrared spectra of $Rh^{I}(CO)_2/Al_2O_3$ before (A) and after (B) UV photolysis. $Rh^{I}(CO)_2$ was formed by exposing 9.2 Torr of CO to a 0.75% $Rh/Al_2O_3$ sample at 300 K for 20 min. Photolysis was carried out in the presence of 2.13 Torr of $C_6H_{12}$ for 5 h with 325 nm UV light at 300 K. Photon fluence = $1.98 \times 10^{21}$ photons $cm^{-2}$. Both spectra were taken with $P < 1 \times 10^{-6}$ Torr. Development of surface-bound $C_6H_{11}$ species is also observed in the C–H stretching region.

h. During the UV photolysis, the temperature of the sample was carefully controlled at 300 K by the combination of electrical heating and cooling. After 5 h of photoreaction, followed by the evacuation of $C_6H_{12}$(g) to $<1 \times 10^{-6}$ Torr at 300 K for 25 min, IR spectra were taken. Figure 1B shows the C–H and C–O stretching regions of the resulting spectra. Two new bands at 2937 and 2864 $cm^{-1}$ were found. They were assigned respectively to the $-CH_2-$ antisymmetric and symmetric stretching mode of the chemisorbed surface cyclohexyl species.[1,2] The assignment of these two bands to the chemisorbed cyclohexyl species is based on the vibrational frequencies which are almost the same as that of gaseous cyclohexane [$\nu(-CH_2-)_{as}$ = 2934 $cm^{-1}$, $\nu(-CH_2-)_s$ = 2861 $cm^{-1}$]. The possibility that these two bands are derived from physisorbed cyclohexane was eliminated by a control experiment (performed under the same temperature, reaction time, and pressure of cyclohexane but without using UV light) which showed no cyclohexyl species on the surface. It was also reported by Ballinger et al.[1,2] that the cyclohexyl is stable on the surface up to 600 K. This further demonstrates that it is a "real" chemisorbed species. Efforts were made to identify the $-CH_2-$ deformation mode of the cyclohexyl species; however, a definite assignment of this mode could not be made.[33]

Accompanying the formation of surface cyclohexyl species, the depletion of $Rh^{I}(CO)_2$ was also observed in Figure 1B. Using the intensity of the 2103-$cm^{-1}$ band, it was estimated that 23% of $Rh^{I}(CO)_2$ was consumed assuming that Beer's law applies for these highly dispersed species. The most distinctive change in the IR spectrum of $Rh^{I}(CO)_2$ was that the symmetric band at 2103 $cm^{-1}$ appears to be depleted faster than the antisymmetric one at 2034 $cm^{-1}$, and this had also been reported previously by Ballinger et al.[1,2] This is due to the fact that during photolysis

(33) A new peak at 1444 $cm^{-1}$ was found after UV photolysis which could be assigned to the $-CH_2-$ deformation mode of chemisorbed cyclohexyl species based on its frequency. However, the same feature accompanying another band at 1660 $cm^{-1}$ was produced on a pure alumina sample after exposure to UV light under vacuum (in the absence of cyclohexane). We believe that these two bands found on the pure alumina are due to a change of the carbonate impurity (which is already present on the alumina obtained from Degussa) after UV exposure. Another photolysis experiment using $Rh^{I}(CO)_2$ was performed with $C_6D_{12}$ in order to avoid the overlapping of the absorption bands of the $-CH_2-$ deformation mode with that of the carbonate mode. A weak $-CD_2-$ antisymmetric stretching band at 2210 $cm^{-1}$ was found; there was nothing observed in the $-CD_2-$ deformation region (~1150 $cm^{-1}$). This can be explained by the fact that the deformation mode of cyclohexane is much weaker than the corresponding stretching mode, and there was only a small amount of cyclohexyl formed on the surface. Also, the infrared absorption cross section of a C–D bond is about 3 to 4 times smaller than that of a C–H bond.

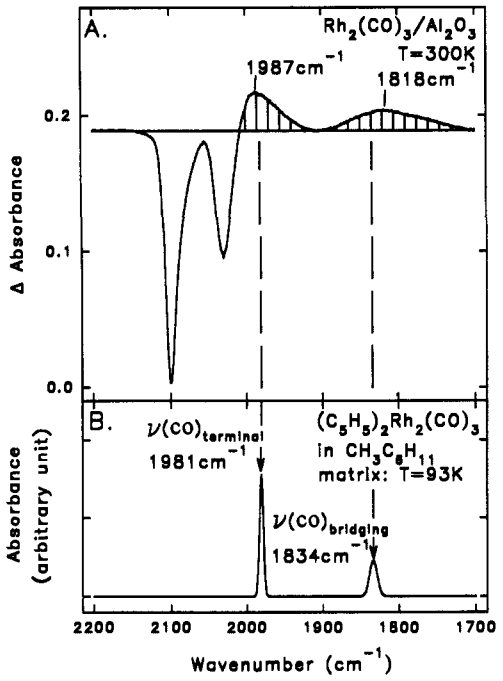


**Figure 2.** (A) The difference spectrum (Figure 1, parts B minus A) after 5 h of photoreaction. The two negative peaks are due to the depletion of $Rh^{I}(CO)_2$. A newly formed surface species, $Rh_2(CO)_3$, was identified by two developing bands at 1987 and 1818 $cm^{-1}$ which are assigned to terminal and bridging CO of $Rh_2(CO)_3$, respectively. The baseline was flattened for display purposes. (B) The IR spectrum of $(C_5H_5)_2Rh_2(CO)_3$ which is analogous to the $Rh_2(CO)_3$ formed on the alumina surface. (Note, only the major CO bands were reproduced from ref 39).

a new IR band develops at about 1990 $cm^{-1}$. Moreover, the intensity of the bridging CO band at about 1820 $cm^{-1}$ in Figure 1 increases 40% from the initial intensity.

**B. Formation of $Rh_2(CO)_3$ Surface Dinuclear Species.** The change in intensity of all of the carbonyl bands may be seen more easily in the difference spectrum, Figure 2A (Figure 1, parts B minus A). Figure 2A shows clearly that the $Rh^{I}(CO)_2$ was depleted with two negative bands at 2103 and 2034 $cm^{-1}$. However, the 2034-$cm^{-1}$ band overlaps with a band developing at 1987 $cm^{-1}$. In addition to the 1987-$cm^{-1}$ band, another carbonyl stretching band at 1818 $cm^{-1}$ was found to develop after UV exposure. We assign these two bands to a new surface species, namely $Rh_2(CO)_3$, which had been formed during UV photolysis. The 1987- and 1818-$cm^{-1}$ bands were assigned respectively to the terminal and bridging C–O stretching modes of $Rh_2(CO)_3$(a). The assignment of these two bands is based on the IR study[34-40] of a similar rhodium compound, dicyclopentadienyltricarbonyldirhodium [$(C_5H_5)_2Rh_2(CO)_3$], also containing terminal and bridging CO bonded to rhodium atoms. Figure 2B shows the IR spectrum (C–O stretching region only) of $(C_5H_5)_2Rh_2(CO)_3$ in a methylcyclohexane matrix at 93 K.[41] The terminal and bridging C–O stretching frequencies (1981 and 1834 $cm^{-1}$ respectively) agree well with that of the adsorbed $Rh_2(CO)_3$ surface species. The peak absorbance ratio of the terminal to bridging CO band [$A(CO)_{terminal}/A(CO)_{bridging}$] in $Rh_2(CO)_3/Al_2O_3$, calculated from the IR spectrum shown in Figure 2A (1.9), is smaller than the

(34) Belt, S. T.; Grevels, F. W.; Klotzbucher, W. E.; McCamley, A.; Perutz, R. N. *J. Am. Chem. Soc.* **1989**, *111*, 8373.
(35) Mills, O. S.; Nice, J. P. *J. Organomet. Chem.* **1967**, *10*, 337.
(36) Herrmann, W. A.; Kruger, C.; Goddard, R.; Bernal, I. *J. Organomet. Chem.* **1977**, *140*, 73.
(37) Hill, R.; Knox, S. A. R. *J. Chem. Soc., Dalton Trans.* **1975**, 2622.
(38) Evans, J.; Johnson, B. F. G.; Lewis, J.; Norton, J. R. *J. Chem. Soc., Chem. Commun.* **1973**, 79.
(39) Evans, J.; Johnson, B. F. G.; Lewis, J.; Matheson, T. W.; Norton, J. R. *J. Chem. Soc., Dalton Trans.* **1978**, 626.
(40) Wrighton, M. S.; Anderson, F. R. *Inorg. Chem.* **1986**, *25*, 112.
(41) The IR spectrum shown in Figure 2B is from ref 40.

**Table 1.** Comparison of CO Vibrational Frequencies ($cm^{-1}$) of Different States of $(C_5H_5)_2Rh_2(CO)_3$ vs $Rh_2(CO)_3/Al_2O_3$

| state | $\nu(CO)_{terminal}$ | $\nu(CO)_{bridging}$ | ref |
|---|---|---|---|
| (1) gas phase | 1990 | 1858 | 29 |
| (2) in cyclohexane solution | 1989 | 1841 | 39 |
| (3) solid in KBr | 1963 | 1816 | 36 |
| (4) matrix: cyclohexane, 93 K | 1981 | 1834 | 40 |
| (5) matrix: 20 K | | | 34 |
| Ar | 1988 | 1844 | |
| $N_2$ | 1986 | 1840 | |
| $CH_4$ | 1985 | 1831 | |
| CO | 1985 | 1832 | |
| (6) in cyclohexane solution | 1984 | 1837 | 34 |
| (7) $Rh_2(CO)_3/Al_2O_3$ | 1987 | 1818 | this work |

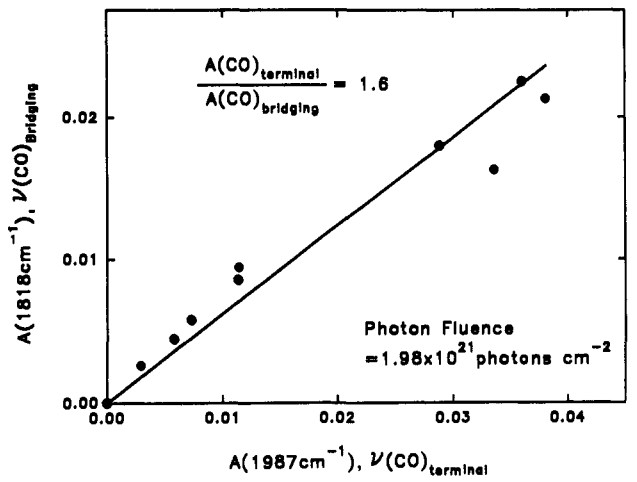


**Figure 3.** Correlation between the bridging and terminal CO absorbance photochemically formed for different Rh loading samples, suggesting that both IR bonds originate from the same species.

expected value (3.4) which is measured from the IR spectrum of $(C_5H_5)_2Rh_2(CO)_3$, Figure 2B. This difference is reasonable because the overlapping of the positive 1987-$cm^{-1}$-difference feature with the negative 2034-$cm^{-1}$-difference feature would yield a smaller absorbance ratio. Moreover, the true frequency of the terminal CO band of $Rh_2(CO)_3/Al_2O_3$ should be higher than 1987 $cm^{-1}$ because of this overlap.

The full widths at half maximum of the carbonyl bands of $Rh_2(CO)_3/Al_2O_3$ are about 10-fold larger than that of the matrix-isolated $(C_5H_5)_2Rh_2(CO)_3$ spectrum shown in Figure 2B. The following explanations may be offered for this: (1) The $(C_5H_5)_2Rh_2(CO)_3$ species is frozen at low temperature in a solid methylcyclohexane matrix, giving sharp IR bands. (2) The inhomogeneous surface of the alumina support results in spectral broadening.

A comparison of IR frequencies for $>Rh_2(CO)_3$ species in different environments is given in Table 1.

The correlation between the production of the 1987-$cm^{-1}$ band (terminal CO) and the 1818-$cm^{-1}$ band (bridging CO) for several different Rh loadings (0.15% to 2.2%, i.e., involving different amounts of $Rh_2(CO)_3$ produced on the alumina) is shown in Figure 3. Even though the 1987-$cm^{-1}$ band is overlapping with the 2034-$cm^{-1}$ band, the peak absorbance of the 1987-$cm^{-1}$ band is almost linearly correlated with that of the 1818-$cm^{-1}$ band in the average ratio of 1.6. This relationship between the terminal and bridging CO bands supports the model that these two bands are derived from the same surface species, $Rh_2(CO)_3$, which are formed during UV photolysis of $Rh^I(CO)_2/Al_2O_3$.

The formation of $Rh_2(CO)_3$(a) from the UV irradiation of $Rh^I(CO)_2/Al_2O_3$ is strongly supported by the fact that a similar rhodium compound, $(C_5H_5)_2Rh_2(CO)_3$ is also produced photochemically from $(C_5H_5)Rh(CO)_2$. Mills and Nice[35] first reported that UV irradiation of $(C_5H_5)Rh(CO)_2$ dissolved in pentane produced $(C_5H_5)_2Rh_2(CO)_3$, a dark red crystal after purification.

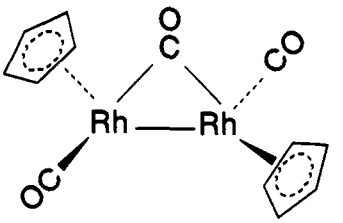


$(C_5H_5)_2Rh_2(CO)_3$

**Figure 4.** Schematic structure of $(C_5H_5)_2Rh_2(CO)_3$ determined by X-ray crystallography.

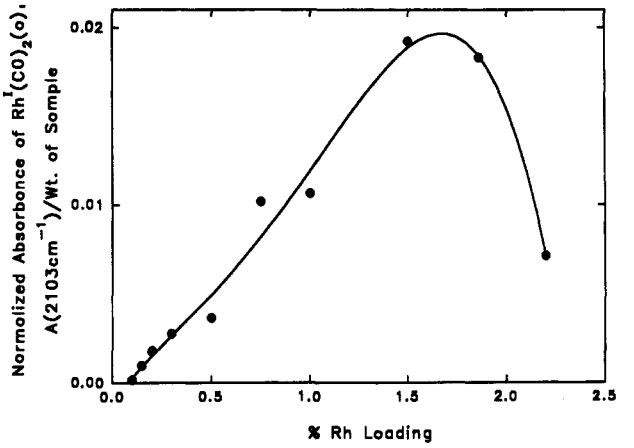


**Figure 5.** Plot of $Rh^I(CO)_2$ formation from CO adsorption as a function of Rh loading on $Al_2O_3$.

The structure of this compound was also determined by X-ray crystallography[35] as shown schematically in Figure 4. Later, Evans,[38,39] Hill,[37] and Herrmann[36] also observed this photochemical reaction. Recently, Bergman[29] reported a gas-phase version of this reaction; the photolysis of $(C_5H_5)Rh(CO)_2$(g) in argon gas at room temperature produced the dinuclear adduct, $(C_5H_5)_2Rh_2(CO)_3$. A very short lived intermediate, $(C_5H_5)Rh(CO)$, was identified in this reaction.

**C. Effect of Rh Loading on the Photochemical Yield of Cyclohexyl Surface Species.** The photochemical activation of cyclohexane experiment was repeated for ten different Rh loadings (0.1, 0.15, 0.2, 0.3, 0.5, 0.75, 1.0, 1.5, 1.86, and 2.2%) under the same experimental conditions as mentioned in section A.

Figure 5 shows the quantitative relationship between the amount of $Rh^I(CO)_2$ formed and the percentage loading of rhodium on alumina. The amount of $Rh^I(CO)_2$ formed was expressed as the peak absorbance of the 2103-$cm^{-1}$ band normalized to the weight of the samples sprayed on the tungsten grid sample holder. Here, the yield of the *gem*-dicarbonyl is almost linearly correlated to the Rh loading up to 1.5%. This plot implies that the number of $Rh^I(CO)_2$ formed per unit area of the support also increases linearly with the Rh loading because of the same specific surface area of the support in all samples. The deviation from linearity at high Rh loading may be explained by the formation of a significant number of large-size Rh crystallites which are not completely converted to the $Rh^I(CO)_2$.

The yield of chemisorbed cyclohexyl surface species after the standard 5 h of UV photolysis as a function of Rh loading ($Rh^I(CO)_2$ surface concentration) is shown in Figure 6. The yield of cyclohexyl was represented by the peak absorbance of the 2937-$cm^{-1}$ band of the cyclohexyl species divided by the initial peak absorbance of the 2103 $cm^{-1}$ band of the $Rh^I(CO)_2$ species. This is equivalent to the relative number of cyclohexyl species produced per unit number of the *gem*-dicarbonyl surface species, the starting material, which is initially present on the surface. This plot shows clearly that the relative yield of the cyclohexyl is low for the

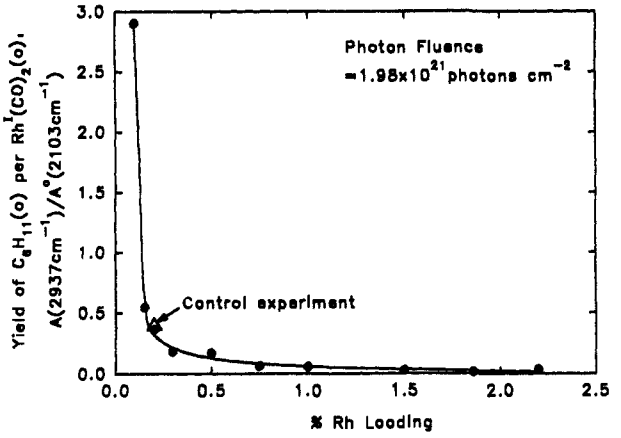


**Figure 6.** Yield of $C_6H_{11}$(a) as a function of Rh loading for identical photon fluence and cyclohexane pressure. The control experiment was performed under excess CO pressure to test whether the buildup of CO pressure during photolysis would retard the production of $C_6H_{11}$(a).

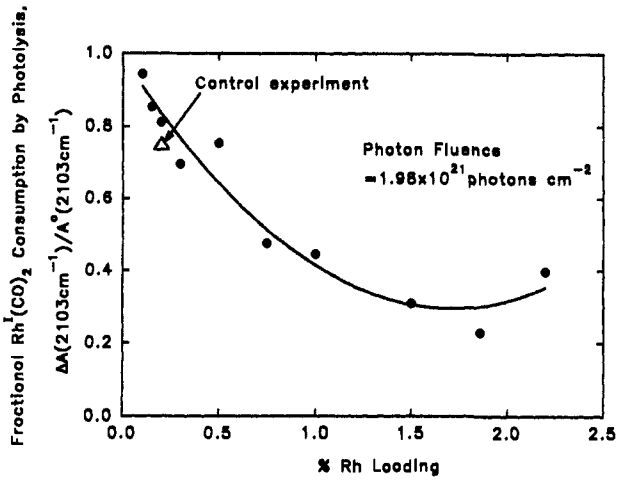


**Figure 7.** Fraction of $Rh^I(CO)_2$ consumed after UV activation in the presence of cyclohexane as a function of Rh loading.

samples having a high surface concentration of $Rh^I(CO)_2$. This observation is just opposite to what is usually expected, i.e., the yield of product increasing with the concentration of reactant. This implies that a competitive side reaction, which significantly reduces the rate of cyclohexane activation, is greatly favored at high surface concentrations of $Rh^I(CO)_2$.

In addition to the yield of cyclohexyl on the surface, the fraction of $Rh^I(CO)_2$ depleted after UV photolysis also demonstrated a Rh loading dependence. Figure 7 shows the relationship between the fractional $Rh^I(CO)_2$ consumption and the Rh loading. A general trend indicating that the fractional consumption of $Rh^I(CO)_2$ decreases with increasing Rh loading is easily seen. This could be explained by the fact that the *gem*-dicarbonyl surface concentration increases with the Rh loading, however, the number of photons per unit area was held constant in all cases. This means the number of photons received by each *gem*-dicarbonyl species decreases with increasing Rh loading and hence the fractional consumption of $Rh^I(CO)_2$ decreases.

Therefore, it is more appropriate to look at the yield of cyclohexyl normalized to the loss of the $Rh^I(CO)_2$ (i.e., the relative number of cyclohexyl species produced per $Rh^I(CO)_2$ species photolyzed) as a function of Rh loading (*gem*-dicarbonyl surface concentration). This is shown in Figure 8. The relative yield was expressed as the peak absorbance of the 2937-$cm^{-1}$ band of the cyclohexyl species divided by the *change of the absorbance* of the 2103-$cm^{-1}$ band of the *gem*-dicarbonyl. Again, a similar trend as shown in Figure 6 was found in Figure 8; the yield of cyclohexyl per $Rh^I(CO)_2$ consumed is also low for the samples with high Rh loading. As mentioned before, this loading effect is likely to be due to a competitive side reaction favored at high Rh loading, i.e. the formation of $Rh_2(CO)_3$(a).

A plot of the formation of $Rh_2(CO)_3$(a) as a function of Rh loading is also shown in Figure 8. The relative yield of $Rh_2(CO)_3$(a) was expressed as the peak absorbance of the 1987-$cm^{-1}$ band of $Rh_2(CO)_3$(a) (measured in difference spectra) divided by the change of peak absorbance of the 2103-$cm^{-1}$ band of the *gem*-dicarbonyl. Figure 8 clearly shows that the yield of the dinuclear surface species $Rh_2(CO)_3$(a) is high for samples of high Rh loading (i.e., high *gem*-dicarbonyl surface concentration). This can be easily understood in the sense that the shorter distance between individual *gem*-dicarbonyl species in high Rh loading samples greatly enhances the probability of the coupling of the transient Rh(CO)(a) species with the $Rh^I(CO)_2$(a) species to form $Rh_2(CO)_3$(a). This coupling suppresses the cyclohexane activation process.

**D. Control Experiment.** It is expected that an equilibrium partial pressure of CO will be attained inside the IR cell (by the photodecomposition of $Rh^I(CO)_2$) during the UV activation. It might be expected that the additional partial pressure of CO would suppress Rh(CO)(a) formation and hence the activation of cyclohexane by this transient species. For high $Rh^I(CO)_2$ coverage, this effect would be expected to increase, and might be responsible for the decrease in the photoyield of cyclohexyl surface species observed. In order to distinguish the CO effect from the $Rh_2(CO)_3$(a) formation effect on the yield of cyclohexyl, a control cyclohexane activation experiment was performed for a low Rh

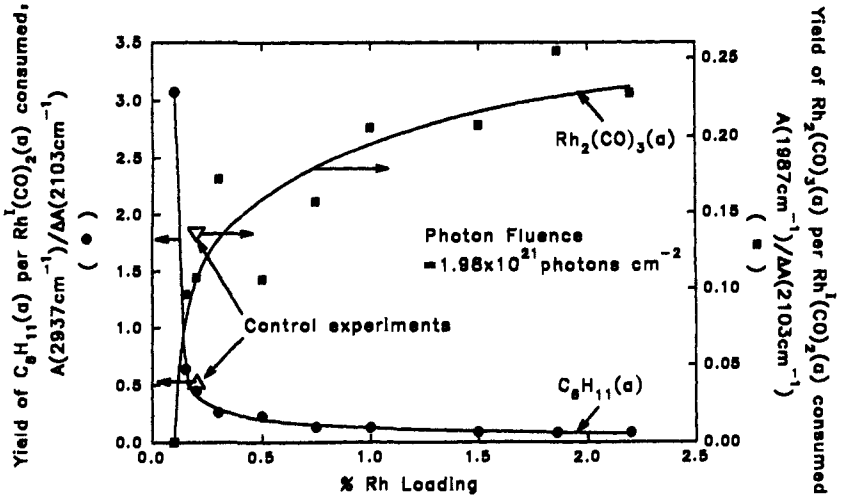


**Figure 8.** Yield of $C_6H_{11}$(a) and $Rh_2(CO)_3$(a) per $Rh^I(CO)_2$ species photochemically consumed after cyclohexane activation as a function of Rh loading.

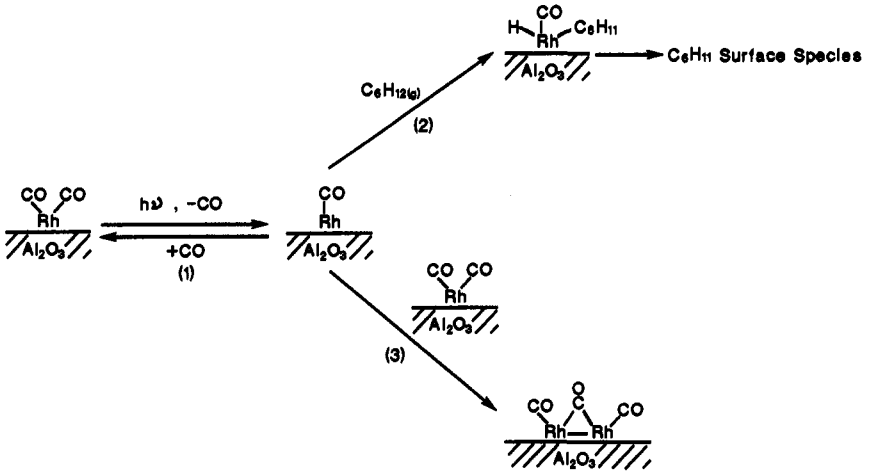


**Figure 9.** Photochemical reaction scheme showing three reaction routes for $Rh^1(CO)/Al_2O_3$ which is produced photochemically from $Rh^1(CO)_2$ on $Al_2O_3$.

loading sample under the same experimental conditions except it was conducted in the presence of both cyclohexane and *added* CO during UV photolysis. If the yield of cyclohexyl of the control experiment was substantially lower than that of a normal experiment at the same Rh loading, it would imply that CO readsorption is at least partially responsible for the effect shown in Figures 6 and 8.

It was found that for a CO-saturated 2.2% $Rh/Al_2O_3$ sample, a 6 mTorr steady state partial pressure of CO(g) was achieved during the photolysis of $Rh^1(CO)_2(a)$ in a closed system. Upon interruption of the photolysis experiment, the photodesorbed CO(g) was observed to readsorb on the surface. A control experiment involving a 0.2% $Rh/Al_2O_3$ sample plus 6 mTorr of CO(g) and 2.12 Torr of cyclohexane was then performed. The result is represented by triangles in Figures 6–8 and shows that the production of CO(g) by the photolysis of $Rh^1(CO)_2$ does not suppress the C–H bond activation observed in these experiments.

## IV. Conclusions

A proposed photochemical reaction scheme for the rhodium *gem*-dicarbonyl species supported on an alumina surface in the presence of cyclohexane is shown in Figure 9. Upon the exposure of $Rh^1(CO)_2(a)$ to UV light, a postulated active surface intermediate, rhodium(I) monocarbonyl, is formed. It undergoes the following reactions: (1) reformation of the rhodium *gem*-dicarbonyl by readsorption of CO; (2) activation of the C–H bonds of cyclohexane by oxidative addition to form $Rh(H)(CO)(C_6H_{11})(a)$ which then produces a stable cyclohexyl surface species; and (3) reaction with a rhodium *gem*-dicarbonyl to form a dinuclear surface species, $Rh_2(CO)_3(a)$, which is inactive for C–H bond activation.

It is proposed that $Rh_2(CO)_3(a)$ formation is a competitive side reaction of the desirable cyclohexane activation process. A competitive relationship between processes (2) and (3), governed by the surface concentration of rhodium *gem*-dicarbonyl, shows that process (2) is suppressed by process (3) at high rhodium *gem*-dicarbonyl surface concentrations.

Control experiments demonstrated that the CO photodesorbed from the rhodium *gem*-dicarbonyl in a closed system has almost no suppressing effect on the activation of cyclohexane when compared to the formation of $Rh_2(CO)_3(a)$.

**Acknowledgment.** This work was supported by the Office of Basic Energy Science, Department of Energy. J. C. S. Wong would also like to thank the Northwest College and University Association for Science (NORCUS) of Washington State University for partial support of a graduate fellowship.